Advances in Environmental Technology 10(1) 2024,70-84.

Iranian Reasearch Organization for Science and Technology (IROST)

Advances in Environmental Technology

Journal home page: https://aet.irost.ir/

Recycling the wasted bentonite clay as a low-cost and novel adsorbent for the removal of the methylene blue dye in the aqueous solution

Mukhtar DH. Shubber[1], Daryoush Yousefi Kebria[2*]

[1] *Ph.D. Student, Department of Environmental Engineering, Babol University of Technology, Iran & Engineer in Directorate of Al-Qadissiyeah environment, ministry of environment,Iraq*

[2] *Associate Professor, Department of Environmental Engineering, Babol University of Technology, Iran*

ARTICLE INFO

Document Type:
Research Paper

Article history:
Received 17July 2023
Received in revised form
1February2024
Accepted 17 February 2024

Keywords:
Adsorption
Bentonite clay waste
Batch System
Methylene Blue dye

ABSTRACT

This study aims to recycle thermal remediated bentonite clay waste (TRBCW) as a green, new, low-cost adsorbent to remove the methylene blue (MB) dye in an aqueous solution. The first system was the batch adsorption experiments having five condition parameters: contact time, pH, temperature, initial concentration of MB, and dose of TRBCW adsorbent. From the analysis of the batch adsorption data, it was apparent that the adsorbing of MB molecules on the TRBCW adsorbent was endothermic, irreversible, promising, spontaneous, and favorable. The Fruendlich model was more compatible than the Langmuir model for the experimental batch adsorption data, and the maximum adsorption capacity was 34.77 mg/g. The second system is the continuous (fixed-bed column) having three investigated condition parameters: the influent MB concentration, flow rate, and (TRBCW weight) bed depth, the adsorption capacity that results from the dominant parameters (1ml/min, 50 mg/L, and 22 cm) was 61.37 mg/g, and the experimental continuous adsorption data were more suitable with Yoon-Nelson, Thomas, and BDST models with R^2> 0.9.

1.Introduction

The development of the industrial sector representing the number and type of factories like a tannery, rubber, paint, pulp, textiles, plastics, and colored paper increases the discharge of industrial wastewater containing different dissolved contaminants like the methylene blue (MB) dye that is the most utilized in the textile industry[1]. Moreover, the (MB) dye is utilized in other fields for medicinal and pharmaceutical industries [2]. Generally, the dyes in the aquatic environment have hurt all living beings due to their ability to reduce the penetration of sunlight, create foul-smelling water, deplete dissolved oxygen, and then disrupt life in aquatic ecosystems [3]. As well as, the MB dye is dangerous due to its

*Corresponding authorTel.: + 9647813100427
E-mail: mukhtardhajir@gmail.com
DOI:10.22104/AET.2024.6356.1741

characteristics, which are cationic and can penetrate and react with some materials[4]. Moreover, the accumulation of MB dye in wastewater leads to several adverse effects on human health, like difficulties in breathing, shock, vomiting, eye burns, cyanosis, diarrhea, tissue necrosis, and nausea[5]. Various advanced techniques to treat industrial wastewater containing MB dye include oxidation, reduction, photochemical degradation, and membrane technology, and the disservices of these methods are high energy demand, elevated cost, and the release of large amounts of hazardous by-products [6-8].The adsorption method is one of the well-known methods that has been applied to remove MB dye due to the low–cost operation, availability, flexibility, and simplicity in the design and operation stage, less releasing for by-products, and the desorption process for some of the adsorbents[9]. Different types of materials can be employed as adsorbents to remove the contaminant of the MB dye from the water with varied maximum adsorption capacities as graphene has 153.85 mg/g [10], the leaves of oil palm have 103.02 mg/g[11], α-chitin nanoparticles have 6.9 mg/g [12], the Fe_3O_4/activated montmorillonite nanocomposite has 106.38 mg/g[13], Activated carbon with sulphuric acid (H_2SO_4) has 12.9 mg/g [14], the extruded pellets of activated lignin-chitosan has 36.25 mg/g [15], a magnetic nano-powder that results from solid waste of the olive industry has 60 mg/g [16], modified activated carbon with anionic has 232.5 mg/g [17], silica-composited biochars have 143.76 mg/g [18]. The adsorbents mentioned were high-cost, complex, and required preparation time. Therefore, converting oily industrial hazardous waste into an adsorbent is distinguished by a low-cost, available, efficient, and high adsorption capacity that will achieve some of the sustainable development goals due to diminishing the negative impacts on the environment and recycling the waste to reduce using the natural sources. The aims of this study is (1) to investigate the efficiency of the (TRBCW) as a green, available, low-cost, environmentally –friendly, and new adsorbent material with high adsorption capacity to remove the methylene blue (MB) dye from aqueous solution via two methods (a) the batch system having various condition parameters as pH, contact time, temperature, the TRBCW adsorbent dose, and the initial concentration of the MB adsorbate, and (b) the bed depth column system with parameters as flow rate, inlet concentration of MB contaminant, and (TRBCW weight) bed depth, (2) analysis the experimental data of both systems with different models of (isotherm, kinetics, and thermodynamic) to identify the optimum parameters and select the most suitable model is more fitting with experimental data.

2. Materials and methods

2.1. Adsorbate and adsorbent materials

The selected adsorbate in this study was the methylene blue (MB) dye with the chemical formula $C_{16}H_{18}ClN_3S.3H_2O$ and MW:373.9 g/mol purchased from BAKER ANALYZED. The composition of the stock solution was by the dissolution of one (1) gm of dry powder of (MB) dye in one liter of distilled water, and then the required concentration was equipped by diluting a specific amount from the original stock. HCl and NaOH with 0.4 N were used to change the pH value of the aqueous solution.The adsorbent was thermal remediated bentonite clay waste (TRBCW), and the origin of this bentonite clay waste is hazardous industrial waste resulting from the factory recycling spent engine oil as in Figure (1.a). Thermal remediation contains two stages: direct burning (the temperature reaches 450±50 ℃) and the electric furnace with 700 ℃ for 100 min to obtain reddish-white powder as in Figure (1.b). More details of the preparation process and the physical and chemical properties of TRBCW adsorbent are in [19]. Some of the significant chemical and physical characteristics of the TRBCW adsorbent are in Table 1.

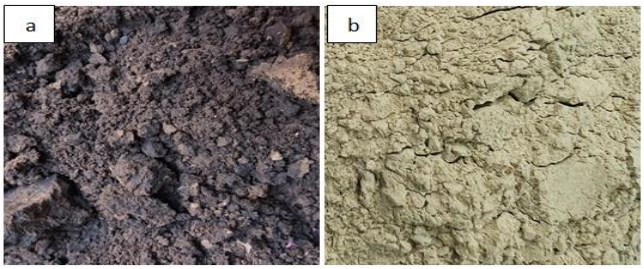

Fig.1. (a) oily industrial solid waste (bentonite clay waste) before thermal remediation, (b) TRBCW adsorbent.

Table 1. The physical and chemical properties of the TRBCW adsorbent [19].

BET test and other features		XRF test	
Specific surface area (m^2/g)	67.17	SiO_2	77.342
pH_{pzc}	10.4	Al_2O_3	10.177
Pore size (nm)	8.54	CaO	5.443
CEC (meq)	22.9	Mg O	3.396
Real density (g/cm^3)	2.133	Fe_2O_3	1.112
Bulk density (g/cm^3)	0.768	SO_3	1.11
Color	Reddish - white	K_2O +Na_2O+ TiO_2	0.913+0.201+0.097

2.2. Adsorption investigations

2.2.1. Batch adsorption system

In the beginning, implementation of the batch adsorption experiments with the five parameters using a graduated container of 100 mL to identify the suitable condition, where the initial pH of the aqueous solution (2, 4, 6.5, 9, and 13), temperature (30, 40, and 50) ℃, contact time (5, 10, 20, 40, 60, 100, and 150) minutes, dose of TRBCW adsorbent (3, 2, 1, 0.5, 0.2, 0.1, and 0.05) g/100 mL, and initial concentration of (MB) dye was (5, 10, 20, 40, 60, 100, and 150) mg/L. The agitation speed of the sample shake was 300 rpm. The selected dominant parameters of pH, contact time, temperature, adsorbent dose, and initial concentration were (6.5, 30 min, 30 ℃, 0.5 g (TRBCW)/100 mL aqueous solution, and 100 mg/L) respectively.

2.2.2. Continuous adsorption system

The investigations of the continuous system via fixed bed depth column principal via Pyrex column 1.06 cm size and its total depth is 44 cm as in Figure 2. Three condition parameters are employed: flow rate (0.5, 1, and 2) mL/min, influent concentration (20, 50, and 100) mg/L, and bed depth (22, 30, and 38) cm resulting from mixing (1, 2, and 3) g from (TRBCW) with (30, 40, and 50) g from quartz sand, respectively to create sufficient permeability and avoid the occurrence of the clogging.The aqueous solution containing the methylene blue was down-flow depending on by-gravity due to the constant pressure principle, where all adsorbent particles of (TRBCW) are immersed in the MB-containing solution to keep the exchange between them and the adsorption process is correct.

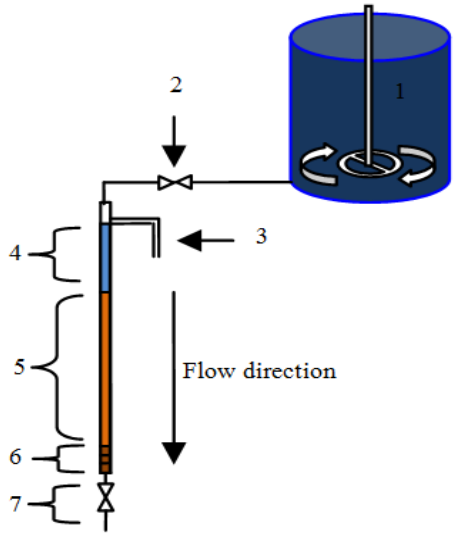

Fig.2. Laboratory set-up of a fixed-bed column system (1) Tank of MB dye solution with agitation motor, (2) Inflow valve, (3) Overflow valve, (4) MB dye solution, (5) Packed column (TRBCW+ sand), (6) Support Layers of quartz sand, and (7) Outflow valve.

2.3. Analytical methods

In the batch system, the adsorption capacity of (TRBCW) and the removal efficiency are identified via formula (1 and 2) [20], respectively.

$$q_e = \frac{Vs\ (C_i - C_e)}{M} \quad (1)$$

$$(R\%) = \left(\frac{C_i - C_e}{C_i}\right) * 100 \quad (2)$$

Where (C_i) and (C_e) (mg/L) are the initial and remaining concentration of methylene blue (MB) dye, (Vs) (mL) is the size of an aqueous solution, M (g) is the adsorbent dose (mass) of (TRBCW).In a fixed bed column system, the total amount of adsorbate interred into the column is m (mg), the adsorbed quantity by (TRBCW) is q (mg), and the removal efficiency (R%) is calculated in equation (3, 4, and 5) [21], respectively. Determination of the times of breakthrough and the exhaustion

depending on the value of the (C_t/C_0) to be equal to 0.05 and 0.8, respectively.

$$m = C_e * Q * t_e \quad (3)$$

$$q = \frac{Q}{1000}\int_0^t (C_0 - C_t)dt \quad (4)$$

$$R\,\% = \frac{q}{m} * 100 \quad (5)$$

Where Q is the flow rate (mL/min), C_t and C_0 (mg/L) are effluent and influent concentrations.MTZ (cm) is the mass transfer zone representing the active bed depth for adsorbing the contaminants through the flowing aqueous solution in the continuous system and is dependent on the total bed depth, the breakthrough time (t_b), and exhaustion time (t_e) as calculated in Equation 6[21]. The standard deviation (Δq%) in equation 7 is a non-linear approach to verify the sufficiency of the models' application and compare the experimental data with the calculated model values[22].

$$\text{MTZ} = \text{total bed depth} * \left(1 - \frac{t_b}{t_e}\right) \quad (6)$$

$$\Delta q\,\% = \sqrt{\frac{\sum[(q_{exp} - q_{cal})/q_{exp}]^2}{Number\ of\ Test - 1}} * 100 \quad (7)$$

2.4. Modeling adsorption data

Modeling the experimental adsorption data is a significant procedure to determine the nature of the adsorption. Therefore, many formulas and equations were employed to analyze the batch adsorption data based on the independent condition parameters like thermodynamic analysis for temperature, isotherm modeling for adsorbent dose and initial concentration of the adsorbate, and kinetic modeling for contact time. The thermodynamic analysis is significant for identifying the effect of temperature on the characteristics of the adsorption process via the value of the enthalpy change (ΔH°), the entropy changes (ΔS°), and standard Gibbs free energy (ΔG°) that are calculated from the below equations[23].

$$K_c = \frac{q_e}{C_e} \quad (8)$$

$$\ln K_c = \frac{\Delta S°}{R} - \frac{\Delta H°}{RT} \quad (9)$$

$$\Delta G° = \Delta H° - T\Delta S° \quad (10)$$

Where (T) in (Kelvin) is absolute temperature, (Kc) is the thermodynamic constant, and (R) is the universal gas constant equal to (8.314 J. mole $^{-1}$. K^{-1}).Kinetic modeling has been utilized to study the behavior of the adsorption process with contact time. Four models are well-known in the adsorption kinetic, the pseudo-first-order (PFO), the pseudo-second-order (PSO), Elovich, and intra-particle diffusion models. However, only PFO in equation 11 [24] and PSO in equation 12 [25] were utilized in this study.

$$\ln(q_e - q_t) = \ln q_t - k_1 t \quad (11)$$

$$\frac{t}{q_t} = \frac{1}{K_2\, q_e^2} + \frac{t}{q_e} \quad (12)$$

The isotherm model is significant in defining the attitude of the adsorption process. Two well-known models in isotherm study are the Langmuir equation 13[26] and the Fruendlich equation 14[27]. Moreover, using the separation factor (RL)in formula 15 that results from the Langmuir model for interpreting the adsorption types, unfavorable (RL > 1), favorable (0 < RL< 1), and linear (RL = 1).

$$\frac{C_e}{q_e} = \frac{1}{q_m * K_l} + \frac{C_e}{q_m} \quad (13)$$

$$\log q_e = \log K_f + \frac{1}{n}\log C_e \quad (14)$$

$$R_L = \frac{1}{1 + K_L * C_0} \quad (15)$$

Where (K_L) is the constant of Langmuir and denote to the adsorption rate, and q_m (mg/g) is the maximum adsorption capacity.K_f is the Fruendlich constant denoting the adsorption capacity, and (1/n) is the heterogeneous factor and represents the adsorption intensity.The continuous adsorption data were analyzed using well-known models like Adams-Bohart, Thomas, Yoon-Nelson, and the bed depth service time (BDST) model as detailed in equations (16, 17, 18, and 18), respectively [28-30].

$$\ln\frac{C_t}{C_0} = K_{AB}C_0\,t - K_{AB}q_{AB}\frac{Z}{F} \quad (16)$$

$$\ln\left(\frac{C_0}{C_t}-1\right) = K_{Th}q_{Th}\frac{m}{Q} - K_{Th}C_0t \quad (17)$$

$$\ln\left(\frac{C_t}{C_0-C_t}\right) = K_{YN}t - \tau K_{TN} \quad (18)$$

$$t_b = \frac{N_0}{C_0U_0}Z - \frac{1}{K_0C_0}\ln\left(\frac{C_0}{C_t}-1\right) \quad (19)$$

Where K is adsorption rate constant, Z is bed depth, (F or U_0) is velocity of flow, λ is the time needed for achieving, (N_0 or q) is the adsorption capacity.

3. Results and discussion

3.1. Standard curve

The measure of the methylene blue dye concentration via the UV-visible spectrophotometer, where the device provides the value of the absorbance and converts it into the equivalent concentration based on the standard curve which was prepared in the laboratory based on the known concentrations as shown in Figure 3. The wavelength of the methylene blue dye was 664 nanometers.

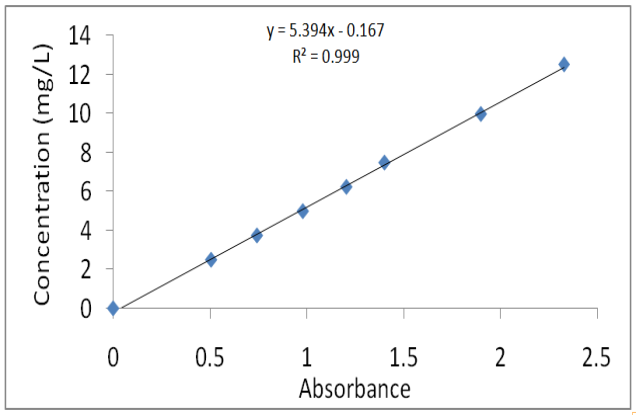

Fig. 3. Standard curve for analysis of methylene blue dye.

3.2. Affecting Factor in Laboratory Work of Batch System

The affecting factors on the adsorption process via the batch approach are initial pH solution (2 to 13), contact time (5 to 150) min, temperature (30 to 50) ℃, the dose of the TRBCW adsorbent (0.05 to 3) g/100 mL, and initial MB dye concentration (5 to 150) mg/L, and the experimental batch adsorption data were studied utilizing adsorption isotherms (Langmuir and Fruendlich model), adsorption kinetics (pseudo-first-order (PFO) and pseudo-second-order (PSO) models), and thermodynamic analysis. The SEM tests in Figure 4 illustrate the variation in the TRBCW adsorbent before and after adsorbing the molecules of MB dye, where the external surface of the TRBCW before adsorption has many separated flakes. However, after the adsorbing and precipitating of the MB dye on the TRBCW surface and filling most of the pores, cavities, and ravines, that led to the variation in the morphology and color of the TRBCW adsorbent. The specific surface area, pore size, and other chemical and physical characteristics in Table 1 were significant factors in increasing the adsorbing molecules of the MB dye.

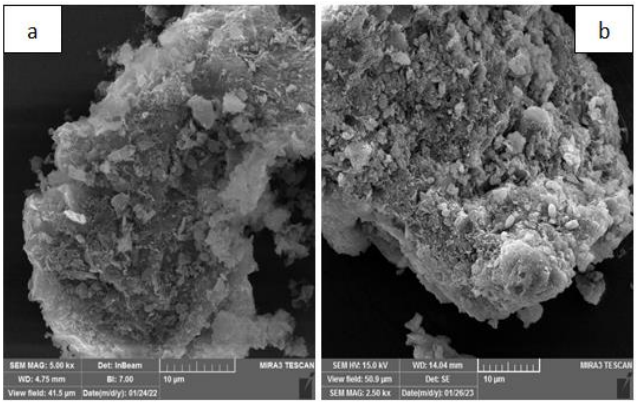

Fig. 4. (a) SEM test for TRBCW before adsorbing, and (b) SEM after adsorbing MB dye.

3.2.1. Initial pH of aqueous solution

Figure (5.a) depicts the role of pH on the (TRBCW) adsorption capacity and the MB dye removal efficiency. Five values of pH were examined (2, 4, 6.5, 9, and 13) where it was apparent that the role of the initial pH value on the results of adsorption capacity (qe) or removal efficiency (R %) was slightly (≈ 6%), and this may be due to that pH_{pzc} of TRBCW was alkaline (10.4) [19] and this can convert the aqueous solution into basic solution. Raising the initial pH value from 2 to 6.5 improves the adsorption capacity slightly from (17.71 to 18.83) mg/g because at a lower initial pH value, the hydrogen ions (H^+) increase and then decrease the entrance of the MB dye cationic to the binding locations of TRBCW due to the rivalry between them towards the active sites of the adsorbent [31], or increase the electrostatic repulsion between them [32]. Moreover, at low initial pH

values, the separation of hydrogen ions (H+) by presenting the functional groups containing oxygen on the TRBCW surface is inferior, and then the electrostatic between the TRBCW and MB dye cationic is lower [17]. The adsorption capacity (qe) decreases after elevating the initial pH value above 6.5, and this lowering is due to the chemical change in methylene blue dye characteristics that result from a decrease in the degree of (MB) dye ionization[33] or ionizable organic components [34], and due to the increase in the repulsion electrostatic between the molecules of MB dye and ions of (OH) [35]on the TRBCW adsorbent surface. The maximum adsorption in the initial pH equaled (≈5.0) and this behavior is similar to that reported in [23].

3.2.2. The dose of TRBCW Adsorbent

The role of the TRBCW adsorbent dose on the adsorption capacity and removal efficiency was evident in Figure (5. b), where the removal efficiency increases from 19.73 % to 98.39 % while the adsorption capacity decreases from (39.46 to 3.28) mg/g when mounting the adsorbent dose from (0.05 to 3) g (TRBCW)/100 mL (solution). Increasing the adsorbent dose means expanding the available surface area and then increasing the number of active locations in the TRBCW surface that is adequate to remove MB dye molecules; Therefore, the start of the adsorption equilibrium state when the removal efficiency of 86.29 % with condition parameters like adsorbent dose reached 0.5 g (TRBCW)/100 mL (solution), initial MB concentration 100 mg/l, contact time 30 min, and initial pH solution 6.5. The equilibrium state indicates that the most active site was binding with dye molecules of MB and the adsorbent dose of 1 g/mL was the optimum adsorbent dose, whereas selecting the adsorbent dose of 0.5 g/100 mL as the dominant parameter in other parameters experiments due to the increasing the adsorbent dose above this value will not achieve a significant change in removal efficiency for dose experiment in addition to the variation in the removal efficiency is more evident for the comparison in the other experiments of pH, temperature, contact time, and initial concentration. The decrease in the adsorption capacity over the unit weight of TRBCW adsorbent with increasing adsorbent weight is yielded from the disability of all molecules of MB dye to bind with all active locations of the TRBCW adsorbent and then achieve the surface equilibrium [17].

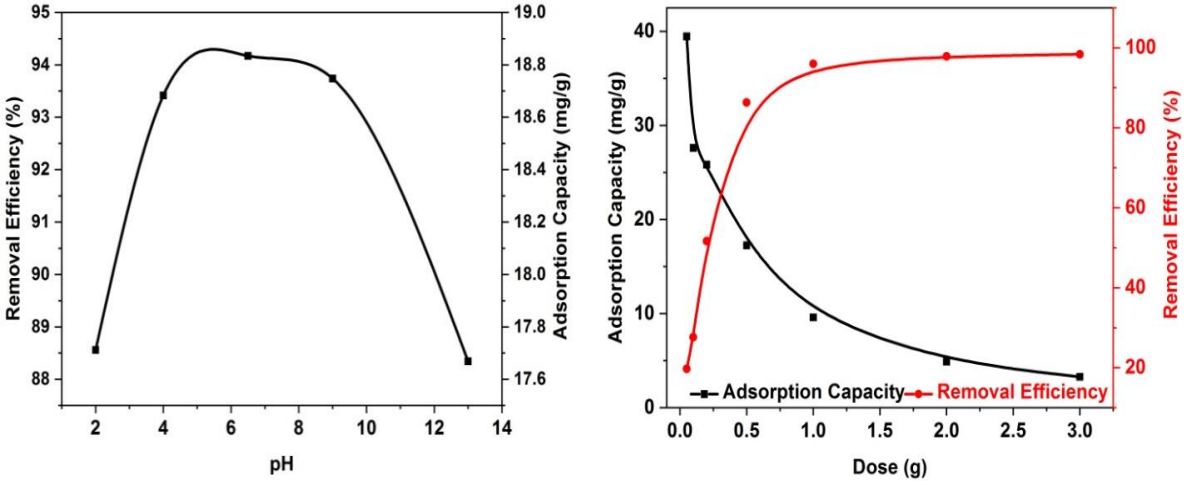

(a) (b)

Fig. 5. The role of (a) pH and (b) the dose of TRBCW adsorbent on the adsorption capacity and removal efficiency.

3.2.3. The temperature effect and analysis of thermodynamic

Figure (6) reveals that the adsorbing of MB dye on the TRBCW surface is endothermic, where it is apparent that elevating the temperature increases the removal efficiency and the adsorption capacity due to a lowering in the solution viscosity and then improves the diffusion speed of MB dye molecules in the direction the exterior layer and interior cavities and pores of TRBCW[37]. Also, increasing the temperature creates an additional number of active locations in the TRBCW adsorbent particles for adsorbing the molecules of MB dye[38]. From the data in Table 2, it was apparent that the

adsorption process of MB dye utilizing the TRBCW adsorbent was endothermic, spontaneous physical adsorption, and irreversible because the values of ΔH°were positive, ΔG° was negative and arranged from (0 to - 20) KJ/mol, and ΔS° being positive[39-40], respectively.

Table 2. Details of thermodynamic analysis.

Temp. (k)	C_e (mg/L)	q_e (mg/g)	Kc	ΔS° (J. K^{-1} mol^{-1})	ΔH° (kJ/mol)	ΔG° (kJ/mol)
303	11.655	17.669	1.516	106.662	31.035	-1.048
313	6.261	18.748	2.994	106.662	31.035	-2.854
323	5.830	18.834	3.231	106.662	31.035	-3.149

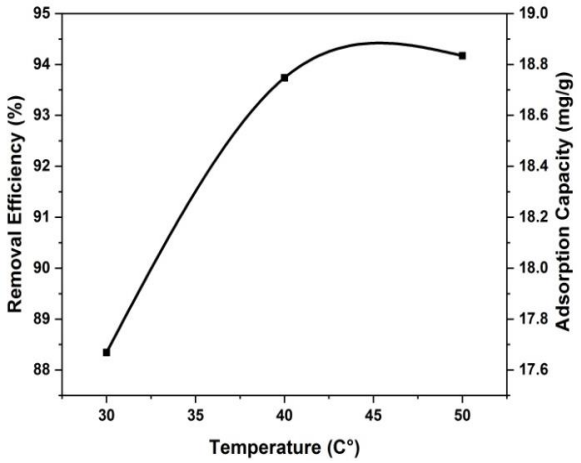

Fig.6. The effect of temperature on the removal efficiency ans adsorption capacity.

for adsorbing the molecules of MB dye[38].From the data in Table 2, it was apparent that the adsorption process of MB dye utilizing the TRBCW adsorbent was endothermic, spontaneous physical adsorption , and irreversible because the values of ΔH° were positive, ΔG° was negative and arranged from (0 to - 20) KJ/mol and ΔS° being positive[39], [40], respectively.

3.2.4. Contact Time and kinetic modeling

The role of contact time on the adsorption capacity(q_e) and removal efficiency (Re %) in the batch adsorption experiments was apparent in Figure (7. a)via various periods (5, 10, 20, 40, 60, 100, and 150) min, it appears that the adsorption capacity improved with advancing contact time from (5 to 60) min with an elevation rate was 15 %. However, the improvement rate in the range from (60 to 150) min was 0.3 %. The improvement rate in the adsorption capacity is high in the first period due to the abundance of active locales in the TRBCW adsorbent [41], and then grow the electrostatic repulsion between the molecules of MB dye that presented on the surface of the TRBCW adsorbent and these in the aqueous solution which leads stabilization in the adsorption efficacy with time progress[42]. The PFO model identifies that the adsorption rate is equivalent (proportional) to the molecules of MB dye (number of adsorbates) that existed in the aqueous solution due to it depends that the diffusion is essential to transporting the molecules from the liquid phase into TRBCW adsorbent surface. The PFO kinetic model indicates that the change in the adsorption rate (k_1) is directly commensurate to the difference between the equilibrium concentration and the adsorbed concentration of the MB dye with time by TRBCW adsorbent regardless of types or the dose of the adsorbent and the adsorption considered as a physical process[24]. The PSO kinetic model exhibits that the adsorption process or contaminants transfer is a chemical reaction that occurs between the TRBCW adsorbent and the adsorbates MB dye, and then the reaction rate (k_2) based on the adsorption capacity (mg/g) and not only on the concentration of MB molecules in aqueous solution[25]. From the results of the analysis in Figure (7.b), it was apparent that PFO was less fitting to the experimental batch adsorption data where the correlation coefficient (R^2) was equal to 0.813 with a standard deviation (Δq%) value equal to 8.492 due to the PFO is suitable only for a first period which is roughly from (20 to 30)min[43]. However, the PSO was more fitting and had an elevated value of (R^2) equal to 0.999 and a low value of the (Δq%) equal to 4.111.

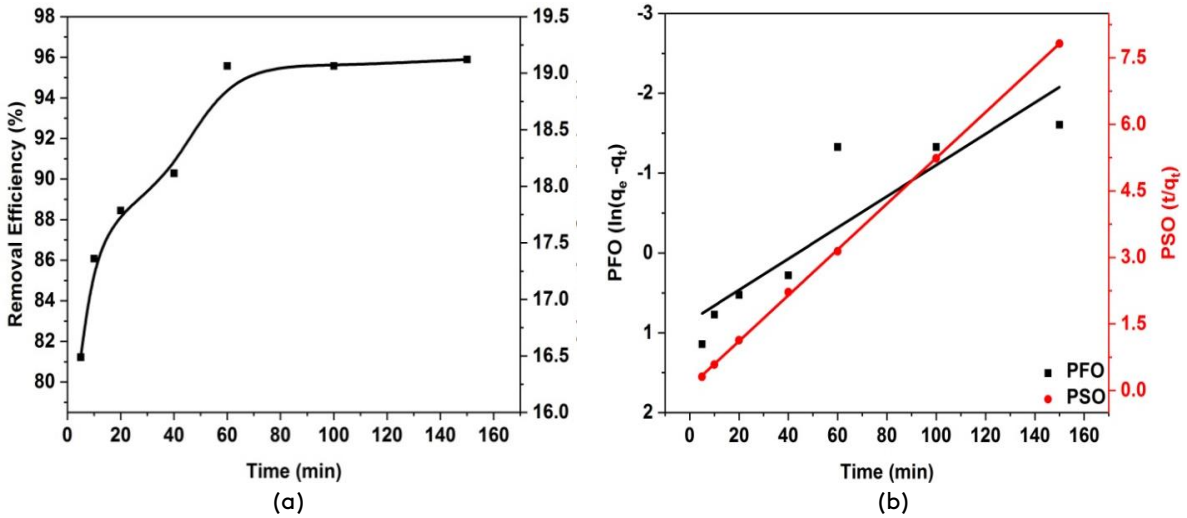

Fig.7. (a) The role of contact time on the (MB dye) removal efficiency and (b) (PFO & PSO) model.

3.2.5. Initial Concentration and adsorption isotherm

The role of the MB dye concentration on the adsorption capacity and removal efficiency was noticeable in Figure (8.a) and is significant for identifying the maximum adsorption capacity(q_m) via TRBCW as adsorbent material. Raising the initial MB dye concentration from (50 to 250) mg/L improves the adsorption capacity from (9.80 to 32.50) mg/g and decreases the removal efficiency (R%) from (98.05 to 65.0) % because an increase in the diffusion of the molecules of MB dye and then increasing the driving force that results from the difference in the concentration level in the solution and on the adsorbent surface[44]. Isotherm analysis is significant for estimating the maximum adsorption capacity by relating the equilibrium concentration to the adsorbent dose with constancy in other parameters like temperature and initial pH solution. Also, identifying the behavior of the adsorption technique and defining the adsorption mechanisms. The Langmuir isotherm supports the principle that one of the active locations of the TRBCW adsorbent can absorb only one of the MB adsorbate molecules, or in other terms, there is a monolayer of adsorbates on the TRBCW adsorbent exterior [26]. Also, it considers that all of the active locations in the TRBCW adsorbent have the same adsorption capacity and no reaction between the MB molecules (adsorbate), and then this leads to the system being homogenous.The Fruendlich isotherm is a practical model that considers that the adsorption is heterogeneous, where it supports that MB dye molecules in this study are in the form of a multilayer on the surface of the TRBCW adsorbent. From the results in Table 3 and Figure (8.b), it was apparent that the Fruendlich model was more fitting with experimental batch adsorption data than the Langmuir model due to the Δq% value being the least although the values of (R^2) are close to others, where the Δq% values were 1.571% and 33.474%, and the values of (R^2) were 0.981 and 0.986 for Fruendlich and Langmuir respectively. The adsorption was favorable due to the (1> RL >0) where the value from (0.153 to 0.035), and the (n) value was equal to 3.608 within (1 to 10), and also, the adsorption was promising due to the value of k_f was 9.348 within the range (1 to 20)[45], [22].

Table 3. the results of Langmuir and the Fruendlich model.

Langmuir parameters	Value	Fruendlich parameters	Value
q_m (mg/g)	34.77	k_f (L/mg)	9.348
$q_{exp.}$ (mg/g)	32.50	n	3.608
k_l	0.110		
R^2	0.985	R^2	0.981
Δq%	33.474	Δq%	1.571

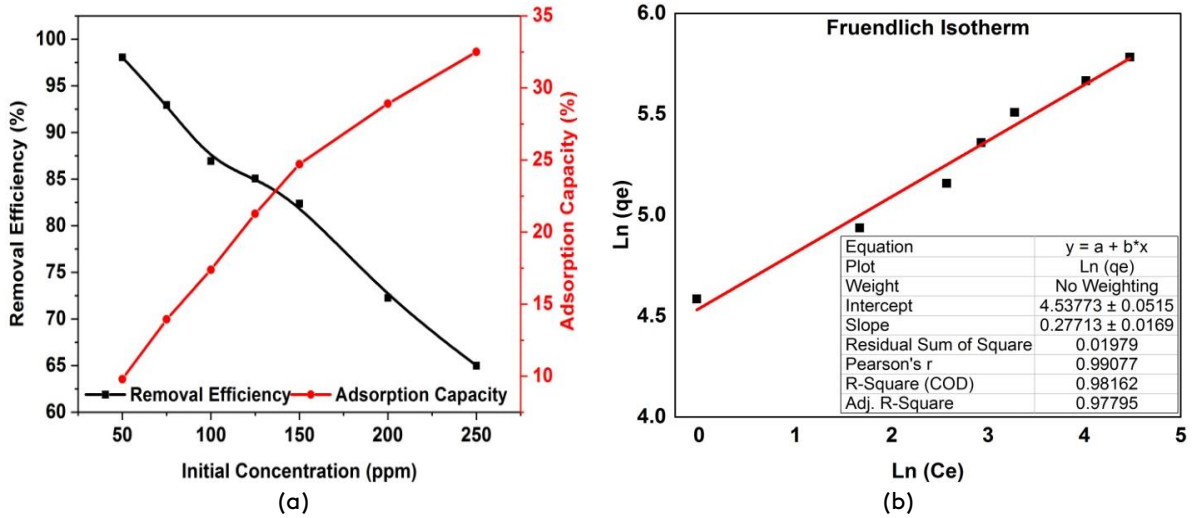

Fig. 8. (a) The role of initial concentration and (b) Fruendlich isotherm.

3.3. Affecting factor in laboratory work of fixed column system

The affecting factors on the adsorption process in the continuous system (fixed bed depth column) are bed depth (weight of the TRBCW adsorbent), influent concentration of MB dye, and flow rate with pH aqueous solution 6.5 and temperature 25± 2 C°. Two models only were drawn for comparison with experimental data, Adams-Bohart and Thomas modeling, where there are no distinctions between the model of Thomas and the models of Yoon-Nelson, and BDST in the drawing due to the similarity of the intercept and slope of them with a difference of signs.

3.3.1. The effect of bed depth

The role of bed depth or weight of the TRBCW adsorbent was evident in Figure (9) and Table 4, three weights of (1, 1.5, and 2) g were mixed with (30, 40, 50) g of sand to produce bed depth of (22, 30, 38) cm, respectively with a flow rate of 1 mL/min and influent MB dye concentration 50 mg/L. It was apparent that mounting the adsorbent weight from (1 to 2) g of the TRBCW adsorbent increased the adsorbed quantity of MB dye from (61.37 to 131.16) mg and the mass transfer zone (MTZ) from (12.30 to 22.12) cm because of an expansion in the TRBCW adsorbent surface area and increasing the number of active locations.Also, increasing the bed depth decreases the axial dispersion rate and increases the axial convection, which is considered a significant factor in increasing removal efficiency, service time, and the mass transfer zone of the column system [46]. It was apparent that an increase in the bed depth of the fixed column decreases the rate constants (K_{AB}), (K_{Th}), (K_{YN}), and (K_0) as in Table 5, and the model adsorption capacity of (q_{AB}), (q_{Th}), (N_0), and also the time (λ) was increase due to the availability of the adsorbing locations result from increase of the bed depth and the length of demand time for adsorbate of (MB) dye to leave the TRBCW bed depth. It was apparent that Thomas, Yoon-Nelson, and BDST models were more fitting with all experimental data as shown in Table 5, where the R^2 values were arranged from (0.90 to 0.98) while the Adams-Bohart model was weak compared with them due to is simulated the experimental data only for an initial period with (C0/Ct < 0.7) [47].

3.3.2. The effect of flow rate

The experiments investigating the role of the flow rate on the adsorbing MB dye were carried out via three levels (0.5, 1, and 2)mL/min, and the effect of this change was evident in the removal efficiency and adsorption capacity, as displayed in Figure (10) and Table 4, where an increase in the flow rate from 0.5 to 2 mL/min decrease the total adsorbed MB dye from (64.12 to 56.28) mg and the removal efficiency from 95% to 61% and increase the MTZ from (11.18 to 16.66) cm. Also, increasing the flow rate decreases the breakthrough and exhaustion time, and then the service time of the column system was shorter, and subsequently, there is more time for the MB molecules to diffuse in the pores and active site of the TRBCW adsorbent. Moreover, the high flow rate decrease from the

adhesion of adsorbates on the surface of the TRBCW adsorbent[48]. It was apparent that an increase in the flow rate increases the rate constants (K_{AB}), (K_{Th}), (K_{YN}), and (K_0) as in Table 5, and the model adsorption capacity of (q_{AB}), (q_{Th}), (N_0), and also the time (λ) decreased due to increase the flow rate increase the number of molecules of MB dye and then the external mass transfer is controlled the kinetic mechanism in the fixed bed depth[49].

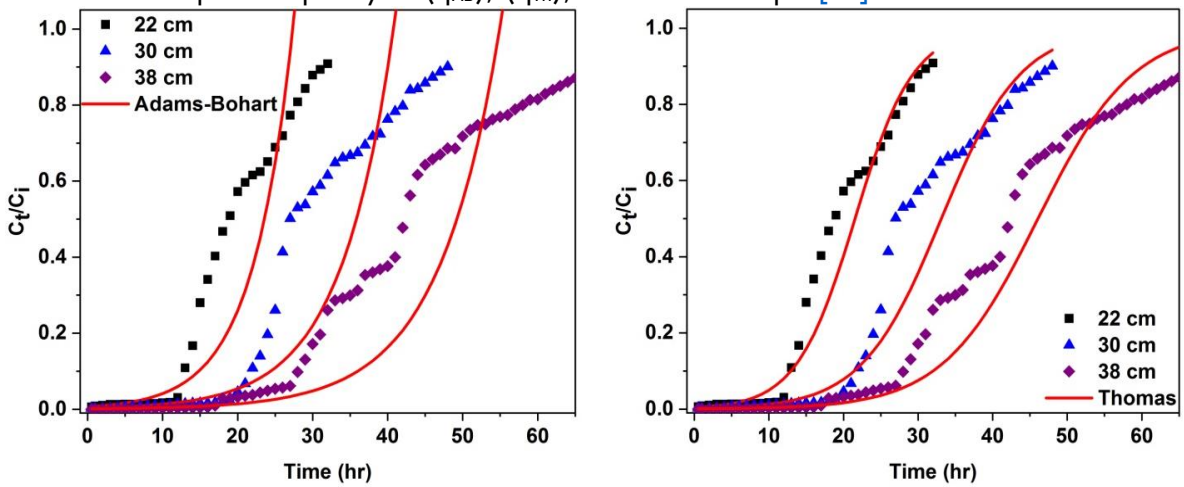

Fig.9. The role of bed depth on the adsorption of MB dye with Adams-Bohart and Thomas modeling.

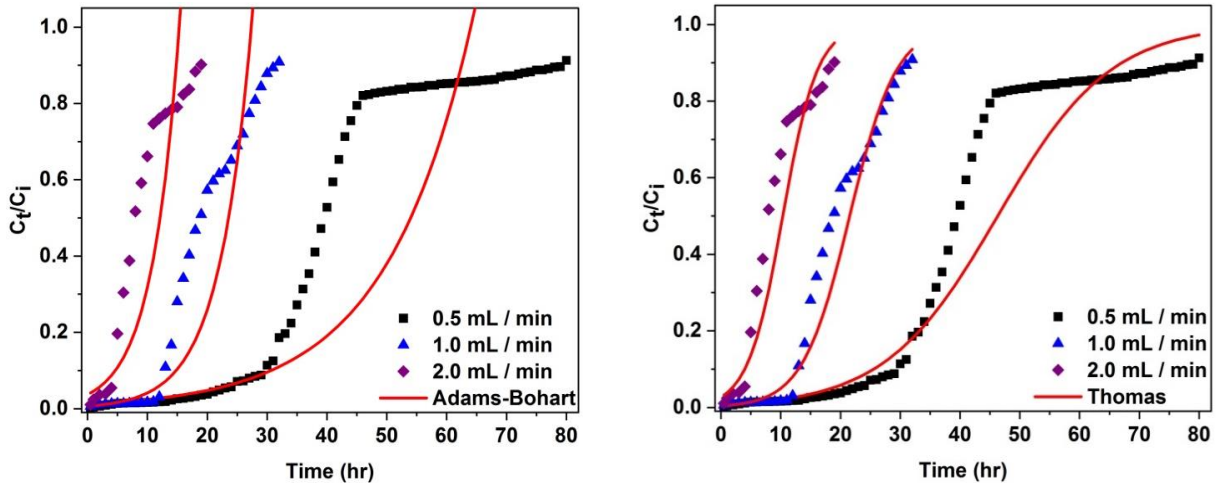

Fig.10. The effect of flow rate on the adsorption of MB with Adams- Bohart and Thomas modeling.

3.3.3. The effect of influent concentration

The role of the influent MB dye concentration was apparent in the change in the removing MB dye from the aqueous solution in a continuous system as in Table 4, as well as the removal efficiency and adsorption capacity curves are in Figure 11, the influent concentration was (20, 50, and 100) mg/L with a flow rate of 1 mL/min and bed depth of 22 cm. It was apparent that the elevating influent MB dye concentration from 20 to 100 mg/L increased the total adsorbed quantity from (48.05 to 80.89) mg and lowered the service time of the column due to the high influent concentration increasing the diffusion of the MB dye molecules in the structure of the column and then available high driving force to achieve fast adsorption[28]. It was apparent that an increase in the influent concentration decreases the rate constants (K_{Th}) and (K_0) and increases (K_{YN}) as in Table 5, and the model adsorption capacity of (q_{AB}), (q_{Th}), (N_0) increase, whereas the time (λ) decreased.

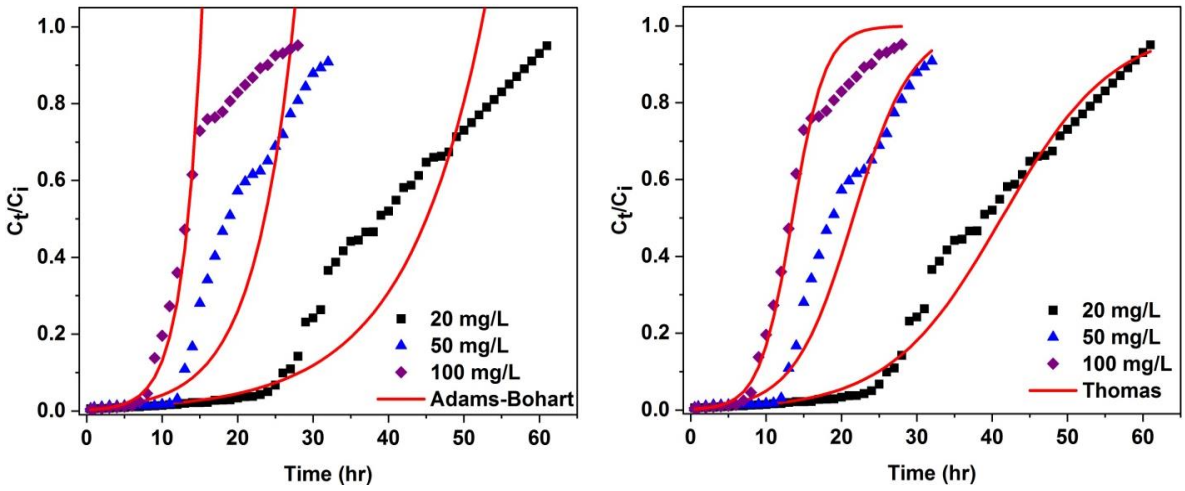

Fig.11. The effect of the influent concentration on the MB dye adsorption with Adams-Bohart and Thomas modeling.

Table 4. the data of experimental work of the MB dye adsorption.

Item	H (cm)	Q (mL/min)	C_i (mg/L)	m (mg)	$q_{exp.}$ (mg)	$q_{exp.}$ (mg/g)	$q_{exp.}$ (mg/l)	R %	Service time (min)	MTZ (cm)
C_{20}	22	1.0	20	64.15	48.05	48.05	2340	74.9	2402	12.1
C_{50}	22	1.0	50	83.27	61.37	61.37	2989	73.7	1227	12.3
C_{100}	22	1.0	100	112.5	80.89	80.89	3939	71.9	809	12.6
$Q_{0.5}$	22	0.5	50	67.80	64.12	64.12	3123	94.6	2565	11.2
Q_2	22	2.0	50	91.75	56.28	56.28	2741	61.3	563	16.7
H_{30}	30	1.0	50	126.2	94.11	62.74	3361	74.6	1882	16.8
H_{38}	38	1.0	50	174.0	131.2	65.58	3698	75.4	2623	22.2

Table 5. The results of the models of MB dye adsorption.

Item	Adams-Bohart			Thomas			Yoon-Nelson			BDST		
	q_{AB} (mg/L)	K_{AB}	R^2	q_{Th} (mg/g)	K_{Th}	R^2	λ (min)	K_{YN} (min^{-1})	R^2	N_0 (mg/L)	K_0	R^2
C_{20}	3055	0.080	0.93	49.5	0.112	0.98	2475	0.002	0.98	2411	0.112	0.98
C_{50}	3996	0.061	0.89	64.6	0.085	0.95	1292	0.004	0.95	3147	0.085	0.95
C_{100}	4443	0.065	0.82	80.9	0.077	0.96	809	0.008	0.96	3941	0.077	0.96
$Q_{0.5}$	4677	0.023	0.86	69.4	0.035	0.92	2778	0.002	0.92	3382	0.035	0.92
Q_2	2594	0.072	0.77	62.1	0.115	0.90	621	0.006	0.90	1750	0.115	0.90
H_{30}	4369	0.047	0.92	66.2	0.063	0.96	1987	0.003	0.96	3548	0.063	0.96
H_{38}	4647	0.041	0.87	69.1	0.052	0.95	2765	0.003	0.95	3897	0.052	0.95

4. Conclusions

- This work studies the ability to use the TRBCW adsorbent as a new, green, available, and low-cost adsorbent for adsorbing MB dye molecules from an aqueous solution. The origin of the TRBCW adsorbent is the thermal remediation of the oily industrial bentonite clay waste produced from the plants recycling spent engine oil with a temperature of 700 °C for 100 minutes.

-It was apparent that the adsorbing of the molecules of MB dye on the TRBCW adsorbent was favorable, promising, endothermic, irreversible, and spontaneous due to the analysis findings of the thermodynamic and isotherm modeling. The maximum adsorption capacity was 34.77 mg/g, and the Fruendlich model was more fitting than the Langmuir model with experimental batch adsorption data. Also, it was apparent from the SEM test that TRBCW adsorbent had high sufficiency to adsorb the MB dye molecules.

- In a fixed column system, with dominant parameters flow rate 1 mL/min, influent MB dye concentration 50 mg/L, and total bed depth 22 cm, the adsorption capacity was 61.37 mg/g, and the service time was 20.45 hr, and the models of Thomas, Yoon-Nelson, and BDST were more fitting with the experimental data than Adams-Bohart model, where the R^2 values of them were > 0.90 due to that the Adams-Bohart was compatible with the first period of the adsorption or with first (20 to 30)min of the operation time.

Recommendations

- Study the capability to modify the adsorbent material (TRBCW) with nano metal oxide particles or functionalize the surface of (TRBCW) with functional groups containing nano-materials or convert them into organic material.
- Study the capability of using prepared TRBCW for removing organic pollutants such as pesticides and phenolic compounds from aqueous solutions in batch and continuous flow systems.

The DOE approach suggested that three parameters, HRT, COD, and biomass concentration, would be significant factors, among which HRT had the most effect. An increase in HRT and/or MLSS enhanced COD removal efficiency, while raising the inlet COD concentration lowered the efficiency. The proposed polynomial model for the prediction of COD removal efficiency had an excellent correspondence with the experimental results. The maximum OLR introduced to the hybrid bioreactor was 3.6 kg COD/ (m^3.d). The data also revealed that the modified Stover–Kincannon highly correlated with the experimental results for the biokinetic modeling of this combined reactor. The modeling demonstrated that by increasing biomass concentration in the biological systems, the biokinetic coefficients increased. In summary, the current combined system could be considered a practical approach to reducing the COD content of beet sugar industry wastewater.

Declaration of competing interest

The authors declare that they have no known competing financial interests or personal relationships that would influence this paper.

References

[1]Mashkoor, F., Nasar, A. (2020). Magsorbents: Potential candidates in wastewater treatment technology–A review on the removal of methylene blue dye. *Journal of magnetism and magnetic materials, 500*, 166408. https://doi.org/10.1016/j.jmmm.2020.166408

[2]El-Kousy, S. M., El-Shorbagy, H. G., Abd El-Ghaffar, M. A. (2020). Chitosan/montmorillonite composites for fast removal of methylene blue from aqueous solutions. *Materials chemistry and physics, 254*, 123236. https://doi.org/10.1016/j.matchemphys.2020.123236

[3]Santoso, E., Ediati, R., Kusumawati, Y., Bahruji, H., Sulistiono, D. O., Prasetyoko, D. (2020). Review on recent advances of carbon-based adsorbent for methylene blue removal from waste water. *Materials today chemistry, 16,* 100233. https://doi.org/10.1016/j.mtchem.2019.100233

[4]Rahman, M. M., Rimu, S. H. (2022). Recent development in cellulose nanocrystal-based hydrogel for decolouration of methylene blue from aqueous solution: a review. *International journal of environmental analytical chemistry, 102*(18), 6766-6783. https://doi.org/10.1080/03067319.2020.1817424

[5]Bayomie, O. S., Kandeel, H., Shoeib, T., Yang, H., Youssef, N., El-Sayed, M. M. (2020). Novel approach for effective removal of methylene blue dye from water using fava bean peel waste. *Scientific reports, 10*(1), 7824. https://doi.org/10.1038/s41598-020-64727-5

[6]Begum, R., Najeeb, J., Sattar, A., Naseem, K., Irfan, A., Al-Sehemi, A. G., Farooqi, Z. H. (2020). Chemical reduction of methylene blue in the presence of nanocatalysts: a critical review. *Reviews in chemical engineering, 36*(6), 749-770. https://doi.org/10.1515/revce-2018-0047

[7]Moradihamedani, P. (2022). Recent advances in dye removal from wastewater by membrane technology: A review. *Polymer Bulletin, 79*(4), 2603-2631.

[8]Ghosh, I., Kar, S., Chatterjee, T., Bar, N., Das, S. K. (2021). Removal of methylene blue from aqueous solution using Lathyrus sativus husk:

adsorption study, MPR and ANN modelling. *Process safety and environmental protection, 149*, 345-361. https://doi.org/10.1016/j.psep.2020.11.003

[9]Meili, L., Lins, P. V. S., Costa, M. T., Almeida, R. L., Abud, A. K. S., Soletti, J. I., Erto, A. (2019). Adsorption of methylene blue on agroindustrial wastes: experimental investigation and phenomenological modelling. *Progress in biophysics and molecular biology, 141*, 60-71. https://doi.org/10.1016/j.pbiomolbio.2018.07.011

[10]Liu, T., Li, Y., Du, Q., Sun, J., Jiao, Y., Yang, G., Wu, D. (2012). Adsorption of methylene blue from aqueous solution by graphene. *Colloids and surfaces B: Biointerfaces, 90*, 197-203. https://doi.org/10.1016/j.colsurfb.2011.10.019

[11]Setiabudi, H. D., Jusoh, R., Suhaimi, S. F. R. M., Masrur, S. F. (2016). Adsorption of methylene blue onto oil palm (Elaeisguineensis) leaves: Process optimization, isotherm, kinetics and thermodynamic studies. *Journal of the Taiwan institute of chemical engineers, 63*, 363-370. https://doi.org/10.1016/j.jtice.2016.03.035

[12]Dhananasekaran, S., Palanivel, R., Pappu, S. (2016). Adsorption of methylene blue, bromophenol blue, and coomassie brilliant blue by α-chitin nanoparticles. *Journal of advanced research, 7*(1), 113-124. https://doi.org/10.1016/j.jare.2015.03.003

[13]Chang, J., Ma, J., Ma, Q., Zhang, D., Qiao, N., Hu, M., Ma, H. (2016). Adsorption of methylene blue onto Fe_3O_4/activated montmorillonite nanocomposite. *Applied clay science, 119*, 132-140. https://doi.org/10.1016/j.clay.2015.06.038

[14]Jawad, A. H., Rashid, R. A., Ishak, M. A. M., Wilson, L. D. (2016). Adsorption of methylene blue onto activated carbon developed from biomass waste by H_2SO_4 activation: kinetic, equilibrium and thermodynamic studies. *Desalination and water treatment, 57*(52), 25194-25206.

[15]Albadarin, A. B., Collins, M. N., Naushad, M., Shirazian, S., Walker, G., Mangwandi, C. (2017). Activated lignin-chitosan extruded blends for efficient adsorption of methylene blue. *Chemical engineering journal, 307*, 264-272. https://doi.org/10.1016/j.cej.2016.08.089

[16]Jodeh, S., Hamed, O., Melhem, A., Salghi, R., Jodeh, D., Azzaoui, K., Murtada, K. (2018). Magnetic nanocellulose from olive industry solid waste for the effective removal of methylene blue from wastewater. *Environmental science and pollution research, 25*, 22060-22074. https://doi.org/10.1007/s11356-018-2107-y

[17]Kuang, Y., Zhang, X., Zhou, S. (2020). Adsorption of methylene blue in water onto activated carbon by surfactant modification. *Water, 12*(2), 587. https://doi.org/10.3390/w12020587

[18]Wang, K., Peng, N., Sun, J., Lu, G., Chen, M., Deng, F., Zhong, Y. (2020). Synthesis of silica-composited biochars from alkali-fused fly ash and agricultural wastes for enhanced adsorption of methylene blue. *Science of the total environment, 729*, 139055. https://doi.org/10.1016/j.scitotenv.2020.139055

[19]Shubber, M. D., Kebria, D. Y. (2023). Thermal recycling of bentonite waste as a novel and a low-cost adsorbent for heavy metals removal. *Journal of ecological engineering, 24*(5), 288-305. https://doi.org/10.12911/22998993/161805

[20]I. Samaka, (2018). Investigate the efficiency of magnetized nanocomposite for sequestration of lead, copper and zinc ions from aqueous solutions. Thesis, Baghdad, Iraq.

[21]Tsai, W. C., de Luna, M. D. G., Bermillo-Arriesgado, H. L. P., Futalan, C. M., Colades, J. I., Wan, M. W. (2016). Competitive fixed-bed adsorption of Pb (II), Cu (II), and Ni (II) from aqueous solution using chitosan-coated bentonite. *International journal of polymer science,* 2016. https://doi.org/10.1155/2016/1608939

[22] Belhadri, M., Mokhtar, A., Meziani, S., Belkhadem, F., Sassi, M., Bengueddach, A. (2019). Novel low-cost adsorbent based on economically modified bentonite for lead (II) removal from aqueous solutions. *Arabianjournal of geosciences, 12*, 1-13. https://doi.org/10.1007/s12517-019-4232-4

[23]Gobi, K., Mashitah, M. D., Vadivelu, V. M. (2011). Adsorptive removal of methylene blue using novel adsorbent from palm oil mill effluent waste activated sludge: equilibrium,

thermodynamics and kinetic studies. *Chemical engineering journal, 171*(3), 1246-1252.
https://doi.org/10.1016/j.cej.2011.05.036

[24]Agbovi, H. K., Wilson, L. D. (2021). Adsorption processes in biopolymer systems: fundamentals to practical applications. *In Natural polymers-based green adsorbents for water treatment,* (pp. 1-51). Elsevier.
https://doi.org/10.1016/B978-0-12-820541-9.00011-9

[25]Sahoo, T. R., Prelot, B. (2020). Adsorption processes for the removal of contaminants from wastewater: the perspective role of nanomaterials and nanotechnology. *In Nanomaterials for the detection and removal of wastewater pollutants*, (pp. 161-222). Elsevier.
https://doi.org/10.1016/B978-0-12-818489-9.00007-4

[26]Rezakazemi, M., Zhang, Z. (2018). 2.29 Desulfurization Materials. *Comprehensive energy systems*, *2*(5), 944-979.
https://doi.org/10.1016/B978-0-12-809597-3.00263-7

[27]Singh, A. K. (2016). Nanoparticle ecotoxicology. Engineered nanoparticles, 343-450.
https://doi.org/ 10.1016/B978-0-12-801406-6.00008-X

[28]Zang, T., Cheng, Z., Lu, L., Jin, Y., Xu, X., Ding, W., Qu, J. (2017). Removal of Cr (VI) by modified and immobilized Auricularia auricula spent substrate in a fixed-bed column. *Ecological engineering,* 99, 358-365.
https://doi.org/10.1016/j.ecoleng.2016.11.070

[29]Al Dwairi, R., Omar, W., Al-Harahsheh, S. (2015). Kinetic modelling for heavy metal adsorption using Jordanian low-cost natural zeolite (fixed bed column study). *Journal of water reuse and desalination, 5*(2), 231-238.
https://doi.org/10.2166/wrd.2014.063

[30]Igberase, E., Osifo, P., Ofomaja, A. (2018). Mathematical modelling of Pb^{2+}, Cu^{2+}, Ni^{2+}, Zn^{2+}, Cr^{+6} and Cd^{+2} ions adsorption from a synthetic acid mine drainage onto chitosan derivative in a packed bed column.*Environmental technology,39*(34),3203-3220.
https://doi.org/10.1080/09593330.2017.1375027.

[31]Sharma, S., Hasan, A., Kumar, N., & Pandey, L. M. (2018). Removal of methylene blue dye from aqueous solution using immobilized Agrobacterium fabrum biomass along with iron oxide nanoparticles as biosorbent. *Environmental science and pollution research*, 25, 21605-21615.
https://doi.org/10.1007/s11356-018-2280-z

[32]Pandey, L. M. (2019). Enhanced adsorption capacity of designed bentonite and alginate beads for the effective removal of methylene blue. *Applied clay science, 169*, 102-111.
https://doi.org/10.1016/j.clay.2018.12.019

[33]Nuengmatcha, P., Mahachai, R., Chanthai, S. (2014). Thermodynamic and kinetic study of the intrinsic adsorption capacity of graphene oxide for malachite green removal from aqueous solution. *Orientaljournal of chemistry, 30*(4), 1463.

[34]Ghadim, E. E., Manouchehri, F., Soleimani, G., Hosseini, H., Kimiagar, S., Nafisi, S. (2013). Adsorption properties of tetracycline onto graphene oxide: equilibrium, kinetic and thermodynamic studies. *Public Library of Science, 8*(11), e79254.
https://doi.org/10.1371/journal.pone.0079254

[35]Li, Y., Wang, M., Sun, D., Li, Y., Wu, T. (2018). Effective removal of emulsified oil from oily wastewater using surfactant-modified sepiolite. *Applied clay science, 157*, 227-236.
https://doi.org/10.1016/j.clay.2018.02.014

[36]De Castro, M. L. F. A., Abad, M. L. B., Sumalinog, D. A. G., Abarca, R. R. M., Paoprasert, P., de Luna, M. D. G. (2018). Adsorption of methylene blue dye and Cu (II) ions on EDTA-modified bentonite: isotherm, kinetic and thermodynamic studies. *SustainableEnvironment research, 28*(5), 197-205.
https://doi.org/10.1016/j.serj.2018.04.001

[37]Güzel, F., Sayğılı, H., Sayğılı, G. A., Koyuncu, F. (2015). New low-cost nanoporous carbonaceous adsorbent developed from carob (Ceratonia siliqua) processing industry waste for the adsorption of anionic textile dye: Characterization, equilibrium and kinetic modeling. *Journal of molecular liquids, 206*,

244-255.
https://doi.org/10.1016/j.molliq.2015.02.037

[38]Singh, K. P., Gupta, S., Singh, A. K., Sinha, S. (2011). Optimizing adsorption of crystal violet dye from water by magnetic nanocomposite using response surface modeling approach. *Journal of hazardous materials, 186*(2-3), 1462-1473.
https://doi.org/10.1016/j.jhazmat.2010.12.032

[39]Nassar, N. N. (2010). Rapid removal and recovery of Pb (II) from wastewater by magnetic nanoadsorbents. *Journal of hazardous materials, 184*(1-3), 538-546.
https://doi.org/10.1016/j.jhazmat.2010.08.069

[40]Kim, Y. S., Kim, J. H. (2019). Isotherm, kinetic and thermodynamic studies on the adsorption of paclitaxel onto Sylopute. The *Journal of chemical thermodynamics, 130*, 104-113.
https://doi.org/10.1016/j.jct.2018.10.005

[41]Liu, L., Zhang, B., Zhang, Y., He, Y., Huang, L., Tan, S., Cai, X. (2015). Simultaneous removal of cationic and anionic dyes from environmental water using montmorillonite-pillared graphene oxide. *Journal of Chemical and Engineering Data*, 60(5), 1270-1278.
https://doi.org/10.1021/je5009312

[42]Shiferaw, Y., Yassin, J. M., Tedla, A. (2019). Removal of organic dye and toxic hexavalent chromium ions by natural clay adsorption. *Desalination and watertreatment, 165*, 222-231.
https://doi.org/10.5004/dwt.2019.24585

[43]Moussout, H., Ahlafi, H., Aazza, M., Maghat, H. (2018). Critical of linear and nonlinear equations of pseudo-first order and pseudo-second order kinetic models. *KarbalaInternational journal of modern science, 4*(2), 244-254.
https://doi.org/10.1016/j.kijoms.2018.04.001

[44]Bulut, Y., Karaer, H. (2015). Adsorption of methylene blue from aqueous solution by crosslinked chitosan/bentonite composite. *Journal of dispersion science and technology, 36*(1), 61-67.
https://doi.org/10.1080/01932691.2014.888004

[45]Batool, F., Akbar, J., Iqbal, S., Noreen, S., Bukhari, S. N. A. (2018). Study of isothermal, kinetic, and thermodynamic parameters for adsorption of cadmium: an overview of linear and nonlinear approach and error analysis. *Bioinorganic chemistry and applications*, 2018.
https://doi.org/10.1155/2018/3463724

[46]Biswas, S., Sharma, S., Mukherjee, S., Meikap, B. C., Sen, T. K. (2020). Process modelling and optimization of a novel Semifluidized bed adsorption column operation for aqueous phase divalent heavy metal ions removal. *Journal of water process engineering, 37*, 101406.
https://doi.org/10.1016/j.jwpe.2020.101406

[47]Ghribi, A., Chlendi, M. (2011). Modeling of fixed bed adsorption: application to the adsorption of an organic dye. *Asian journal of textile, 1*(4), 161-171.

[48]Futalan, C. M., Wan, M. W. (2022). Fixed-bed adsorption of lead from aqueous solution using chitosan-coated bentonite. International *Journal of environmental research and public health, 19*(5), 2597.
https://doi.org/10.3390/ijerph19052597

[49]Kundu, S., Gupta, A. K. (2007). As (III) removal from aqueous medium in fixed bed using iron oxide-coated cement (IOCC): experimental and modeling studies. *Chemical engineering journal, 129*(1-3), 123-131.
https://doi.org/10.1016/j.cej.2006.10.014

How to site this paper:

Shubber, M. (2024). Recycling the wasted bentonite clay as a new and low-cost adsorbent for the removal of the methylene blue (MB) dye from the aqueous solution.*Advances in Environmental Technology*,10(1), 70-84. doi: 10.22104/aet.2024.6356.1741